

## Functionalized Mesoporous Carbons as Platinum Electrocatalyst Supports for Applications in Fuel Cells

Shou-Heng Liu\*, Jyun-Ren Wu

Department of Chemical and Materials Engineering, National Kaohsiung University of Applied Sciences, Kaohsiung 80778, Taiwan

\*E-mail: [shliu@kuas.edu.tw](mailto:shliu@kuas.edu.tw)

Received: 21 June 2012 / Accepted: 27 July 2012 / Published: 1 September 2012

---

Mesoporous carbons (MCs) were synthesized by an organic-organic self-assembly process and surface-modified by the conventional acid-oxidation, H<sub>2</sub>O<sub>2</sub> oxidation and 3-[2-(2-aminoethylamino)ethylamino]propyltrimethoxysilane (AEPTMS) grafted methods. Fabrication of Pt nanoparticles (NPs) supported on MC (Pt/MC) and modified MC (Pt/MC-HNO<sub>3</sub>, Pt/MC-H<sub>2</sub>O<sub>2</sub> and Pt/MC-AEPTMS) were further performed. These resultant catalysts were characterized by a variety of different spectroscopic and analytical techniques such as Fourier transformation infrared spectroscopy (FTIR), X-ray diffraction (XRD), and transmission electron microscopy (TEM) analysis. Pt NPs were found to be aggregated on the Pt/MC-HNO<sub>3</sub> catalysts. For Pt/MC-AEPTMS catalysts, Pt NPs (ca. 2 nm) supported uniformly on surface of modified MC which however has a low electrical conductivity. Among three surface-modified methods, the H<sub>2</sub>O<sub>2</sub> treatment method was a simply controllable way for surface modification of MC which possesses desirable electrical conductivity, well-dispersed and nanosized Pt (ca. 3 nm). The Pt/MC-H<sub>2</sub>O<sub>2</sub> samples were found to have superior electrocatalytic activity for oxygen reduction reaction in comparison with synthesized Pt/MC, Pt/MC-HNO<sub>3</sub>, Pt/MC-AEPTMS and the typical commercial electrocatalyst (Pt/XC-72).

---

**Keywords:** Platinum, Mesoporous carbon, Surface modification, Oxygen reduction reaction.

### 1. INTRODUCTION

Highly dispersed noble metal (Pt) nanoparticles (NPs) supported on conductive materials with high surface areas, such as carbon blacks [1-5], carbon nanotubes [6-9], graphene [10,11] and mesoporous carbons (MCs) [12-16] are desirable for anodic/cathodic electrocatalysts in direct methanol fuel cells (DMFCs) and proton-exchange membrane fuel cells (PEMFCs). Generally, surface functionalization of carbon supports may increase the surface binding sites, avoid metal NPs aggregation, and improve the dispersion of metal NPs. Nevertheless, it is also certainly accompanied

with some problems, such as irregular distribution of the surface functional groups, structural damage, and partial loss in electrical conductivity of the carbon supports.

In the previous studies, we have developed a novel route to fabricate well-dispersed and highly stable mono- (Pt) and bi-functional (PtCo) NPs (ca. 2-3 nm) supported on MCs based on the nano-casting method [17-22]. The synthesized Pt and PtCo/MC catalysts were found to possess superior electrocatalytic performances compared to most commercially available cathodic electrocatalysts (Pt on XC-72 activated carbons). However, the synthesis routes invoked in above-mentioned electrocatalysts were still limited by the ineffectiveness in material cost and preparation time, which further hinder their practical industrial applications. In recent years, fabrication of MCs by cross-linking phenolic resins in the presence of various self-assembled block-copolymer templates, followed by pyrolysis at moderate temperature, have been extensively studied [23-25]. The resultant MCs were found to possess high surface areas with ordered mesopores and structure matrices abundant with hydroxyl groups that facilitate further surface functionalization by dispersion/loading of catalysts in a controllable fashion. In the present study, a simple procedure was developed to synthesize MC by one-step self-assembly approach. Moreover, the synthesized MC materials were treated with various chemical modifications, including  $\text{H}_2\text{SO}_4/\text{HNO}_3$ ,  $\text{H}_2\text{O}_2$  oxidation and 3-[2-(2-aminoethylamino)ethylamino]propyltrimethoxysilane (AEPTMS) functionalization. After incorporating Pt NPs, the resultant Pt/MC and Pt/modified MC samples were examined as electrocatalysts for oxygen reduction reaction (ORR) at cathode by electrochemical techniques, aiming to improve the electrocatalytic activity.

## 2. EXPERIMENTAL

### 2.1. Catalyst Preparation

The MC samples were synthesized by dissolving 3.2 g of phloroglucinol (98%, Acros) and 5.0 g of F127 tri-block copolymer (Sigma) in 36.0 g of ethanol and water mixture (1:1 vol%). After the complete dissolution of the solid ingredients under stirring at room temperature (298 K), 0.4 g of HCl (37 wt%) was added into the solution as a catalyst, then, the mixture solution was further stirred for 2 h. Subsequently, 5.0 g of formaldehyde (37 wt%) was slowly introduced dropwisely into the above solution. The resultant solution was kept for 24 hr after which two separate layers were readily observed. After discarding the upper solution layer, the lower polymer-rich layer was cured at 373 K for 24 hr, followed by a gradual carbonization treatment (1 K/min) under vacuum to 1123 K and maintained at the same temperature for additional 3 h. Surface modifications of MC were performed in three ways. (1) Acid oxidation of MC was carried out by refluxing MC samples in a mixed acid solution ( $\text{H}_2\text{SO}_4$  :  $\text{HNO}_3$  in volume ratio of 1) at room temperature for 4 hr. (2) MC samples were also refluxed with  $\text{H}_2\text{O}_2$  at 353 K for 4 hr. Then, both of treated MC samples were washed with deionized water, filtered and dried at room temperature. (3) The MC samples were functionalized with AEPTMS by a postgrafting method. Typically, MC samples were refluxed in toluene solution containing AEPTMS at 383 K for 24 hr under an  $\text{N}_2$  flow. The products were washed with toluene and dried at

333 K overnight. Pt NPs were deposited on the surface-modified MC by using wet chemical reduction method [26]. In brief, ca. 0.1 g of  $\text{H}_2\text{SO}_4/\text{HNO}_3$ ,  $\text{H}_2\text{O}_2$  and AEPTMS-treated samples were added in a solution containing a desired amount of 0.01 M hydrogen hexachloroplatinate hexahydrate ( $\text{H}_2\text{PtCl}_6 \cdot 6\text{H}_2\text{O}$ , Acros). The mixture was stirred for 30 min and an excessive 0.1 M sodium boronitride ( $\text{NaBH}_4$ , Aldrich) solution was added into the mixture dropwisely. After stirring for 1 hr, the solid was recovered by centrifugation, extensively washed with  $\text{H}_2\text{O}$  and dried in air at 333 K for 24 hr. The obtained samples were denoted as Pt/MC- $\text{HNO}_3$ , Pt/MC- $\text{H}_2\text{O}_2$  and Pt/MC-AEPTMS, respectively.

## 2.2. Characterization methods

The amounts of platinum in various samples were analyzed by energy dispersive X-ray analysis (EDX, JEOL JEM-2100F). All powdered X-ray diffraction (PXRD) patterns were recorded on a PANalytical (X'Pert PRO) diffractometer using  $\text{CuK}\alpha$  radiation ( $\lambda = 0.1541$  nm). Nitrogen adsorption isotherms were measured at 77 K on a Micromeritics ASAP 2020 analyzer. Fourier transform infrared (FTIR) spectra were collected on a Bio-rad 165 spectrometer with  $4\text{ cm}^{-1}$  resolution using KBr pellets at room temperature. For the transmission electron microscopy (TEM), samples were first suspended in acetone (99.9 vol%) by ultrasonication, followed by deposition of the suspension on a lacey carbon grid, then the TEM images were obtained at room temperature using an electron microscope (JEOL JEM-2100F) operating at an electron acceleration voltage of 200 kV. The electrical conductivity ( $\sigma$ ) of samples was conducted according to the method reported in the literature [27].

## 2.3. Electrocatalytic performance

The electrocatalytic measurements were performed in a single compartment glass cell with a standard three-electrode configuration. A glassy carbon electrode (diameter ca. 5 mm) was used as a working electrode and a saturated Ag/AgCl electrode and a platinum wire were used as reference and counter electrodes, respectively. In this study, all potentials are referred to the reversible hydrogen electrode (RHE). The glossy carbon thin-film electrode was prepared by the following steps: first, ca. 5 mg of Pt-loaded carbon sample was added into 2.5 mL deionized water, followed by ultrasonic treatment for 0.5 h. Then, ca. 20  $\mu\text{L}$  of the resultant suspension mixture was withdrawn and injected onto the glassy carbon electrode, followed by drying in air at 333 K for 1 h. Finally, 20  $\mu\text{L}$  of 1% Nafion<sup>®</sup> (DuPont) solution was added as a binder under  $\text{N}_2$  environment. Electrocatalytic activity measurements of various Pt/MC and modified Pt/MC samples were performed on a potentiostat/galvanostat (CHI Instruments, 727D). Cyclic voltammetry (CV) experiments were performed to clean and activate the electrode surface. Prior to each CV measurement, the electrolytic solution was purged with high-purity  $\text{N}_2$  (99.9%) for at least 0.5 h to remove the dissolved oxygen, subsequently the experiment was conducted between 0 and 1.2 V under purging  $\text{N}_2$  condition. Oxygen reduction reaction was evaluated by a linear sweep voltammetry (LSV) technique. The 0.1 M  $\text{H}_2\text{SO}_4$  electrolyte was saturated with ultrahigh purity oxygen for at least 0.5 h. T The polarization curves were

obtained between 0.1 and 1.0 V vs. RHE at a scanning rate of 5 mV/s and a rotating speed of 1600 rpm under room temperature condition.

### 3. RESULTS AND DISCUSSION

Surface modifications of MC were investigated by Fourier transformation infrared spectroscopy (FTIR). Fig. 1 shows that pristine MC possessed a weak and broad band at ca.  $3400\text{ cm}^{-1}$  was attributed to the presence of O-H groups on the surface of the MC which may be due to the moisture bound to MC. In the FTIR spectrum of the oxidized MC by using  $\text{H}_2\text{SO}_4/\text{HNO}_3$  and  $\text{H}_2\text{O}_2$ , a weak feature at ca.  $1720\text{ cm}^{-1}$  is attributed to the C=O stretch of the carboxylic groups [28]. Additionally, an apparent band at ca.  $3400\text{ cm}^{-1}$  was observed for oxidized MC, which also can be ascribed to O-H stretching vibrations of carboxylic groups. Moreover, the FT-IR spectrum obtained from MC-AEPTMS samples suggested the presences of N-H and C-N vibrations at ca.  $1643$  and  $1150\text{ cm}^{-1}$ , respectively. This result indicated that AEPTMS was successfully grafted onto the surface of MC.

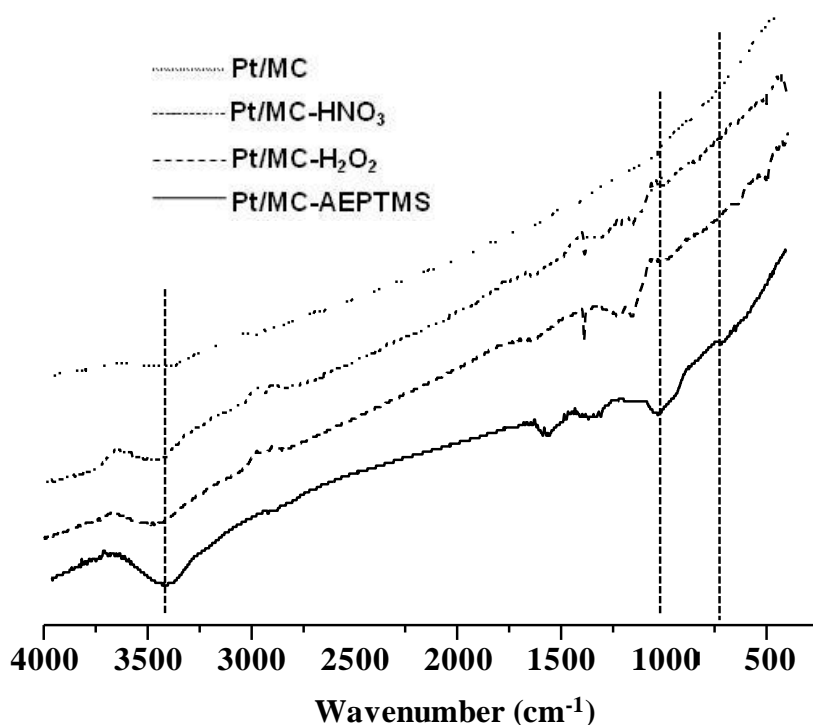


**Figure 1.** FT-IR spectra of various samples.

As shown in Fig. 2, a broad diffraction peak at ca.  $24.6^\circ$  is attributed to C (002) of MC samples. Upon loading Pt NPs onto MC and modified MC samples, the large-angle XRD patterns show distinct (111), (200), (220), and (311) diffraction peaks at  $2\theta = 39.8^\circ$ ,  $46.2^\circ$ ,  $67.8^\circ$ , and  $81.3^\circ$ , respectively, in accordance with those of Pt metal NPs with a face-centered cubic (fcc) structure. According to Scherrer formula, the average sizes of Pt deduced from the XRD profiles of Pt/MC, Pt/MC- $\text{HNO}_3$ , Pt/MC- $\text{H}_2\text{O}_2$  and Pt/MC-AEPTMS samples were found to be 4.5, 6.6, 3.0 and 2.2 nm (see Table 1),

respectively, indicating the Pt particle size can be reduced as the surfaces of MC were modified using H<sub>2</sub>O<sub>2</sub> and AEPTMS.

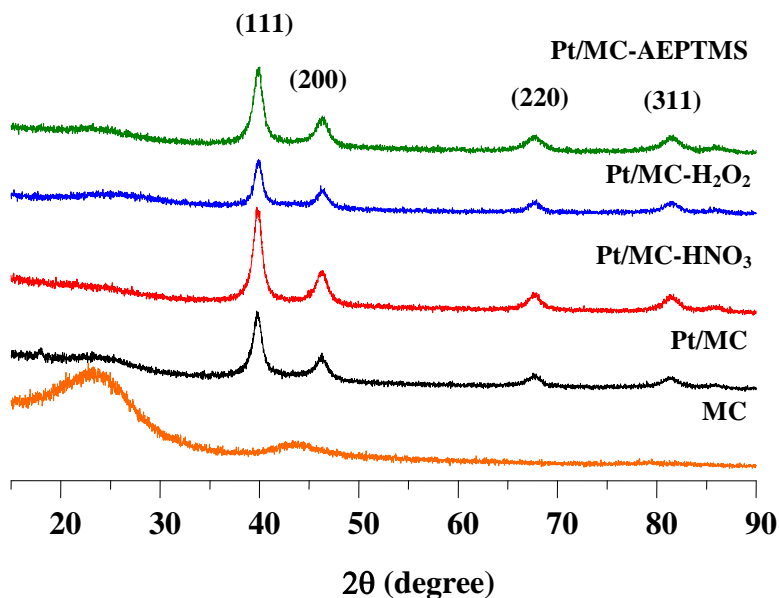


Figure 2. Powdered XRD patterns of various samples.

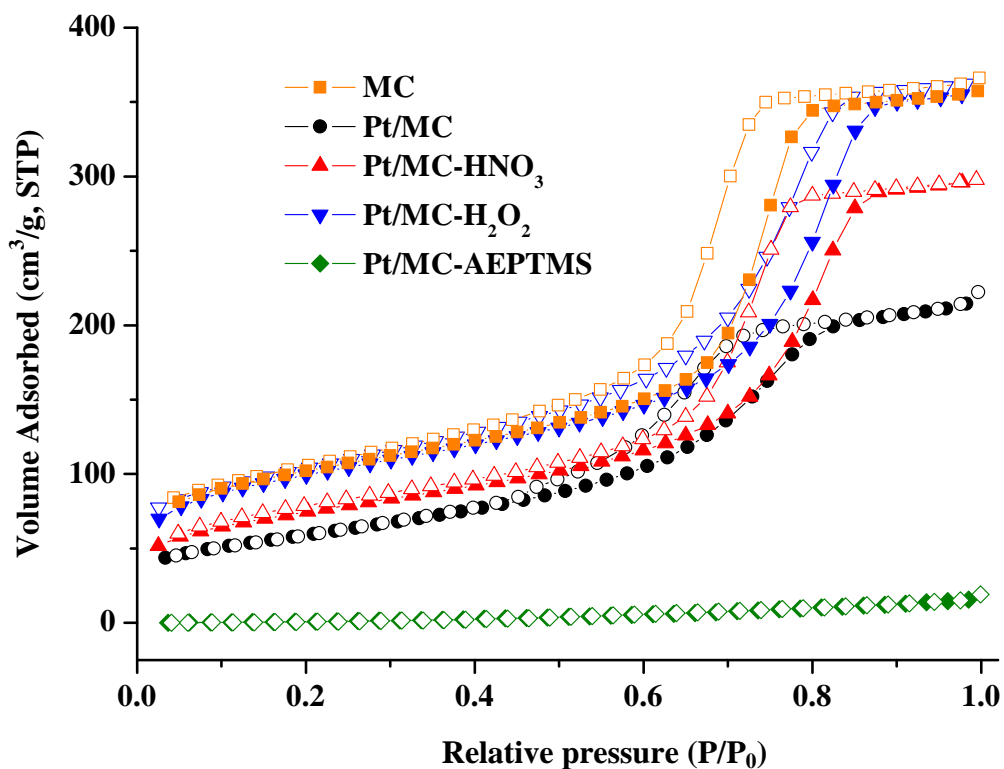


Figure 3. N<sub>2</sub> adsorption/desorption isotherms of various samples.

N<sub>2</sub> adsorption/desorption curves of various samples suggested the typical type-IV isotherm with a well-defined hysteresis loop, as displayed in Fig. 3. Nonetheless, Pt/MC-AEPTMS samples

possess a nearly null  $N_2$  uptake, indicating an excessive AEPTMS loading resulting in lack of porosity with a low surface area ( $S$ ) of only ca.  $53 \text{ m}^2$ . As a result, their structural parameters of various samples are summarized in Table 1. MC samples were found to possess a high BET surface area ( $347 \text{ m}^2 \text{ g}^{-1}$ ) and a uniform pore size distribution (9 nm). However, the average pore sizes ( $D_{\text{BJH}}$ ), surface areas ( $S_{\text{BET}}$ ) and pore volumes ( $V_{\text{tot}}$ ) observed for Pt/MC and Pt on modified MC catalysts are decreased, which may be due to at least two possibilities: (1) porous structure of MC may be partially distorted by severely chemical treatments; (2) the partial blockage of mesopores by higher density of Pt NPs.

**Table 1.** Physical properties of MC and various Pt/MC samples.

sample	Pt (wt%)	$S_{\text{BET}}^{\text{a}}$ ( $\text{m}^2 \text{ g}^{-1}$ )	$D_{\text{BJH}}^{\text{b}}$ (nm)	$V_{\text{tot}}^{\text{c}}$ ( $\text{cm}^3 \text{ g}^{-1}$ )	$D_{\text{p}}^{\text{d}}$ (nm)	$\sigma^{\text{e}}$ ( $\text{S cm}^{-1}$ )
MC	--	347	9	0.56	--	14.6
Pt/MC	13.0	205	7	0.35	4.5	17.5
Pt/MC- $\text{HNO}_3$	14.9	211	9	0.36	6.6	7.7
Pt/MC- $\text{H}_2\text{O}_2$	15.1	305	6	0.43	3.0	4.5
Pt/MC-AEPTMS	13.1	53	6	0.14	2.2	1.1

<sup>a</sup>BET surface area. <sup>b</sup>BJH pore diameter. <sup>c</sup>Total pore volume. <sup>d</sup>Average crystallite size deduced by the Scherrer formula based on the (220) diffraction peak in Fig. 2. <sup>e</sup>Electrical conductivity.

The structure of MC and dispersions of Pt NPs on modified MC samples were studied by TEM measurements. The corresponding particle size distribution histograms were also obtained by calculating the size of more than one hundred randomly selected particles in the magnified TEM images. As displayed in Fig. 4, the bright-field TEM images of Pt/MC, Pt/MC- $\text{H}_2\text{O}_2$  and Pt/MC-AEPTMS samples show their characteristic mesoporous structures. Nevertheless, the hazy image was observed for acid oxidation-treated samples (Pt/MC- $\text{HNO}_3$ ), indicating severe structural damage caused by oxidation of strong acids. Pt NPs with an average size of ca. 5.1 nm in Pt/MC samples were aggregated to some extent. In particular for Pt/MC- $\text{HNO}_3$ , the distribution of Pt was very inhomogeneous, accordingly, formation of Pt aggregates ( $> 10 \text{ nm}$ ) was observed. As can be seen in Pt/MC- $\text{H}_2\text{O}_2$  and Pt/MC-AEPTMS samples, Pt NPs were dispersed uniformly with average sizes of 3.2 and 2.3 nm, respectively, suggesting that surface treatments by  $\text{H}_2\text{O}_2$  and AEPTMS were favorable for well-dispersed Pt NPs on MC. Interestingly, it was found that the average particle sizes calculated by TEM are slightly larger than those obtained from XRD result by Scherrer's formula, as shown in Table 1. This may be due to the miss counting of smaller NPs inside the pore channels.

To investigate the electrocatalytic activities of Pt/MC, a commercially available JM-Pt/C (Johnson-Matthey; 20 wt% Pt on Vulcan XC-72 activated carbon) and various Pt on modified MC materials during ORR, we have performed a series of linear scanning voltammetry (LSV) tests for these samples in  $\text{O}_2$  saturated 0.1 M  $\text{H}_2\text{SO}_4$  solution at room temperature (298 K). As can be seen in Fig. 5, an onset potential of ca. 0.90 V was observed for the Pt/MC catalyst. A decrease in onset potential (0.88 V) corresponding to the Pt/MC-AEPTMS sample was evident for its low electrical conductivity ( $1.1 \text{ S cm}^{-1}$ , see Table 1) even if small Pt particle size and good Pt dispersion were found.

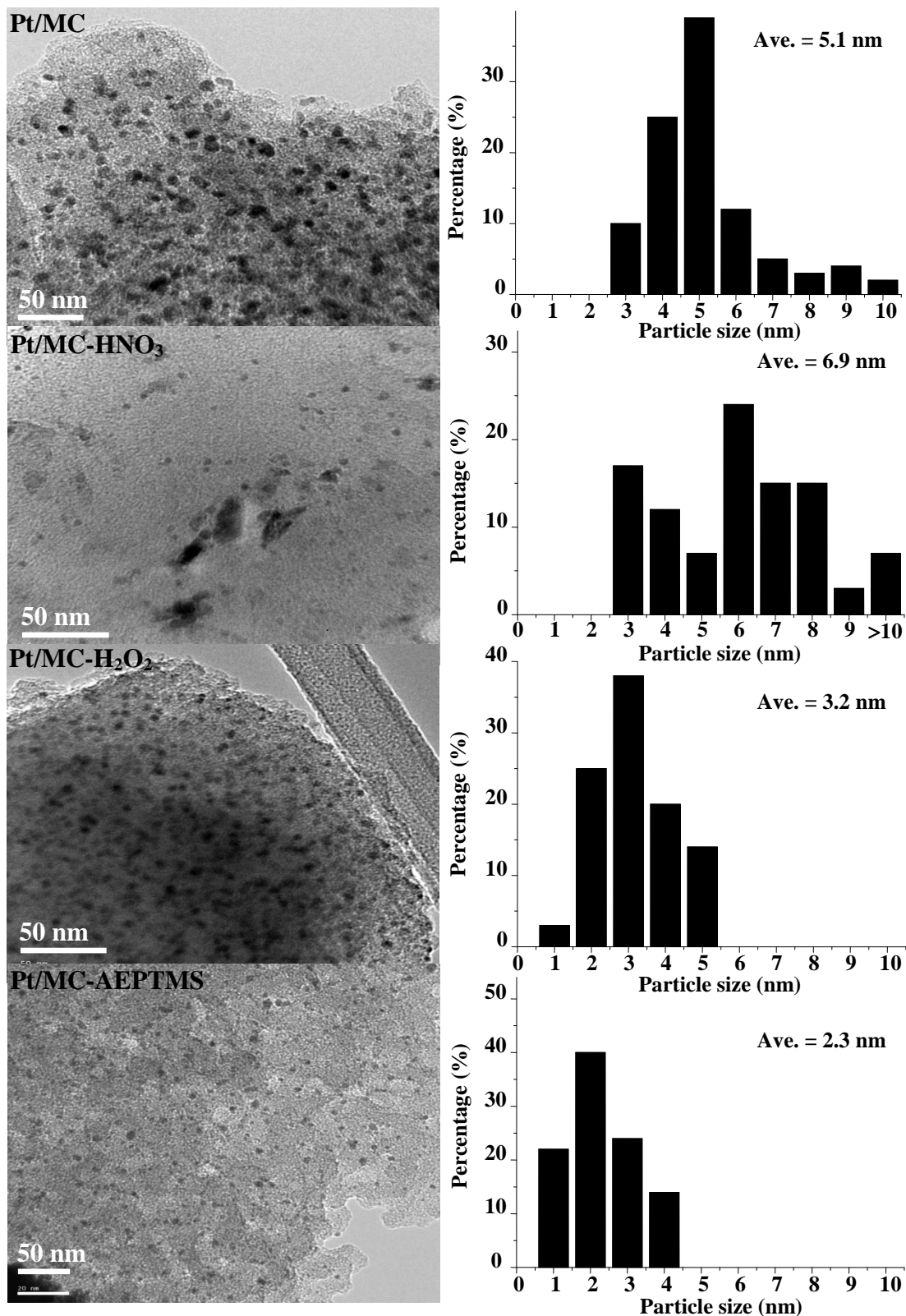


**Figure 4.** TEM images and their corresponding histograms of Pt particle size distributions of various samples.

Among the Pt/modified MC catalysts, Pt/MC-H<sub>2</sub>O<sub>2</sub> was found to possess the best ORR electrocatalytic performance (onset potential = 0.95 V) surpassing that of the commercial JM-Pt/C

catalyst (0.90 V). This can be attributed to the well-dispersed and nanosized (ca. 3 nm) Pt supported on the H<sub>2</sub>O<sub>2</sub>-modified MC with moderate electrical conductivity (4.5 S cm<sup>-1</sup>).

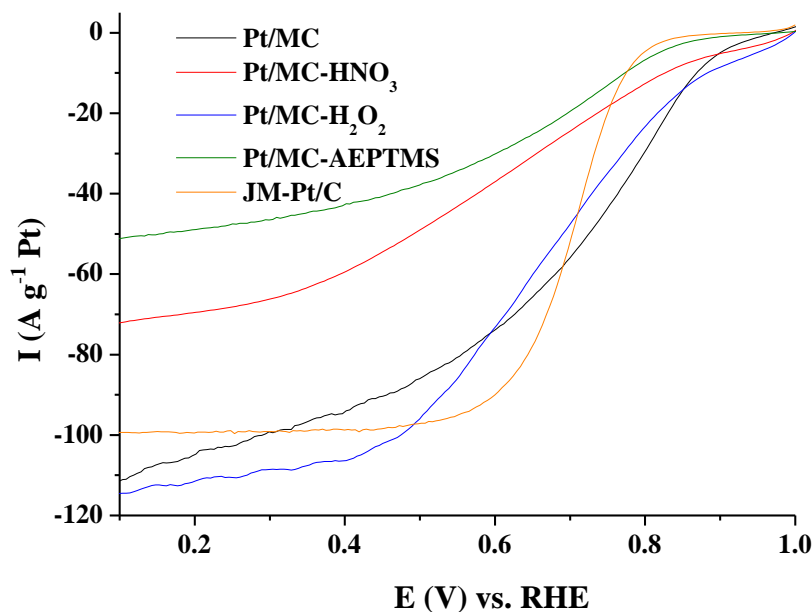


**Figure 5.** Polarization curves during oxygen reduction for various samples in O<sub>2</sub> saturated 0.1 M H<sub>2</sub>SO<sub>4</sub> solution at room temperature.

The reaction mechanisms invoked during ORR over various Pt/MC and Pt/modified-MC electrocatalysts were further explored quantitatively by rotating disk electrode (RDE) voltammetry. In particular, the number of exchanging electrons involved in electron transfer during the ORR process may be obtained from the Koutecky-Levich first-order reaction equation [29,30]:

$$j^{-1} = j_k^{-1} + j_{dl}^{-1}$$

where  $j$  is the measured current density,  $j_k$  is the kinetic current density for the ORR, and  $j_{dl}$  is the diffusion-limiting current density that can be expressed by the following equations:

$$j_{dl} = B\omega^{1/2}$$

$$B = 0.62nFC_{O_2}D_{O_2}^{2/3}\nu^{-1/6}$$

where  $B$  represents the Levich slope,  $\omega$  denotes the rotating angular frequency,  $n$  is the number of the exchange electrons during the ORR process,  $F$  is Faraday constant,  $C_{O_2}$  and  $D_{O_2}$  respectively represents the concentration and diffusion coefficient of oxygen dissolved in the electrolyte, and  $\nu$  is the kinematic viscosity of the electrolyte. The parameters used in this calculation were based on experimental data reported earlier [31-33].

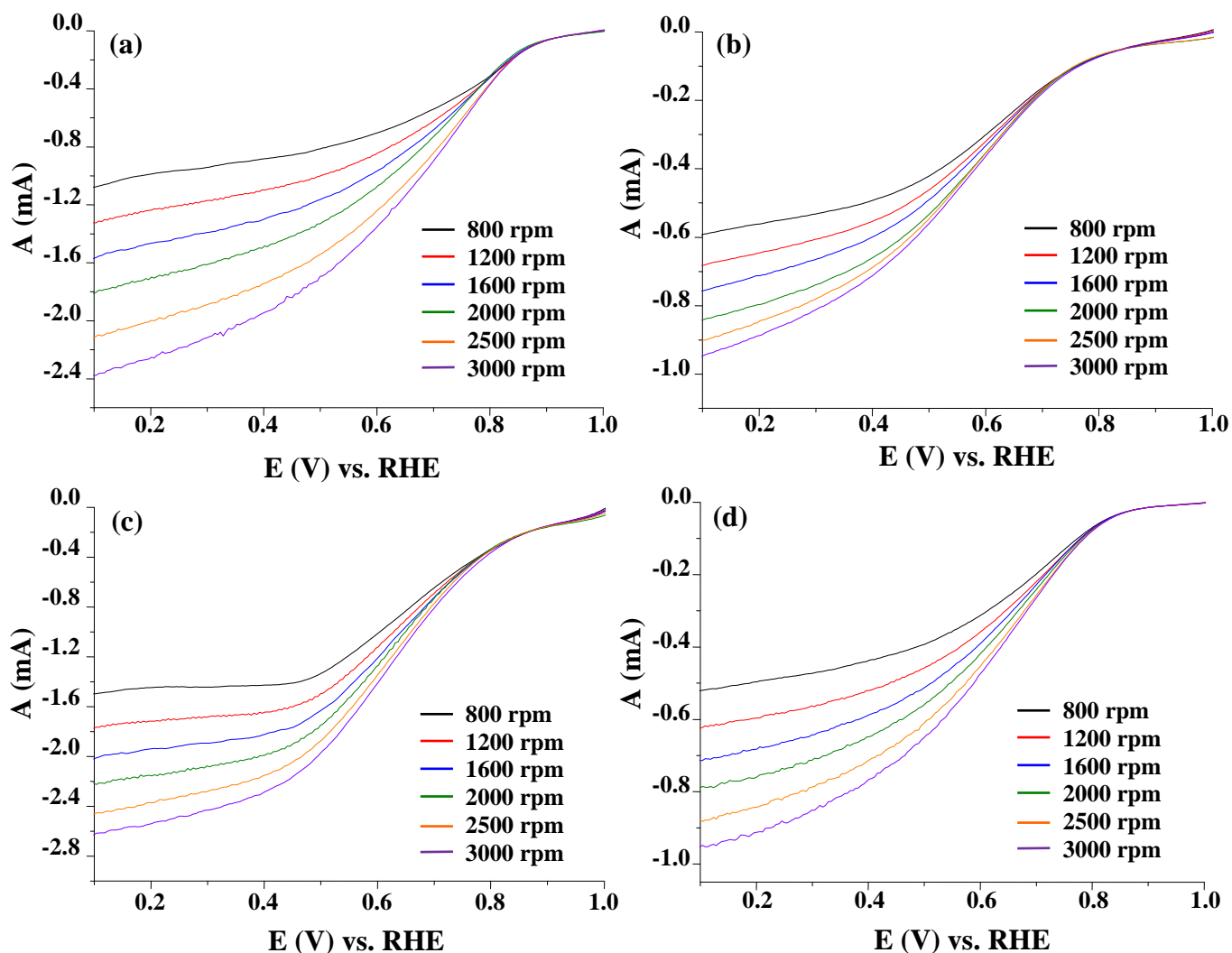


**Figure 6.** Oxygen reduction reaction on (a) Pt/MC, (b) Pt/MC-HNO<sub>3</sub>, (c) Pt/MC-H<sub>2</sub>O<sub>2</sub> and (d) Pt/MC-AEPTMS electrode in O<sub>2</sub> saturated 0.1 M H<sub>2</sub>SO<sub>4</sub> solution at room temperature and different rotating rates.

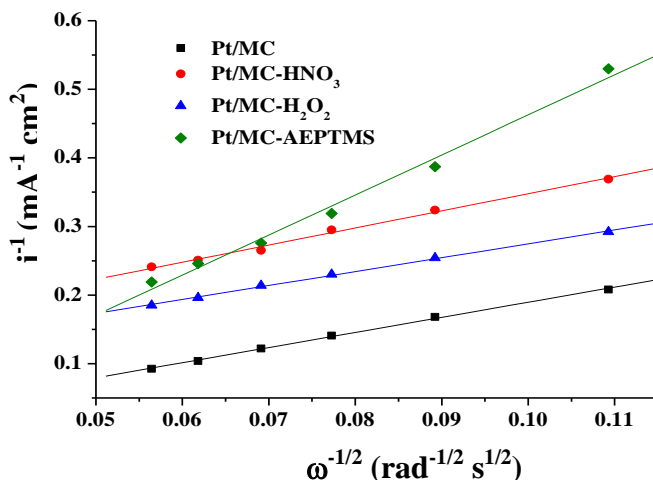


**Figure 7.** Koutecky-Levich plots during ORR for various catalysts at 0.3 V vs RHE in O<sub>2</sub> saturated 0.1 M H<sub>2</sub>SO<sub>4</sub> solution at room temperature.

Various RDE voltammograms of various Pt/MC and Pt/modified-MC electrocatalysts in O<sub>2</sub> saturated 0.1 M H<sub>2</sub>SO<sub>4</sub> solution at room temperature under different rotating rates are illustrated in Fig. 6, and their corresponding Koutecky-Levich plots at 0.3 V vs. RHE are shown in Fig. 7. Accordingly, the number of electron (n) involved during ORR in the Pt/MC, Pt/MC-HNO<sub>3</sub> and Pt/MC-H<sub>2</sub>O<sub>2</sub> electrocatalysts were deduced to be 4.1, 3.9 and 4.2, respectively, close to the theoretical value (4.0) for reduction involving four-electron transfer. However, Pt/MC-AEPTMS had the n value of 2.5, which was also responsible for the worst ORR activity among all electrocatalysts. It is known that two-electron reductions during ORR lead to production of hydrogen peroxide radicals which attack the carbon support as well as the proton exchange membrane (PEM) electrolyte, resulting in an undesirable degradation of the membrane-electrolyte-assembly (MEA) of the fuel cells.

#### 4. CONCLUSIONS

In summary, three surface-modified routes including H<sub>2</sub>SO<sub>4</sub>/HNO<sub>3</sub>, H<sub>2</sub>O<sub>2</sub> oxidation and AEPTMS functionalization were studied by using self-assembly MC as carbon supports. Pt deposition on H<sub>2</sub>O<sub>2</sub>-treated MC surface using H<sub>2</sub>PtCl<sub>6</sub> precursors by wet chemical reduction process was a controllable and simple way to optimize a cathodic catalyst during ORR. Thus, Pt/MC-H<sub>2</sub>O<sub>2</sub> which possessed moderate electrical conductivity, well-dispersed and nanosized Pt (ca. 3 nm) was found to have surpassing ORR electrocatalytic activity as compared to Pt/MC, Pt/MC-HNO<sub>3</sub>, Pt/MC-AEPTMS and a commercial JM-Pt/C catalyst. These Pt/MC-H<sub>2</sub>O<sub>2</sub> should render practical cost-down effective commercial applications in hydrogen energy related areas, for examples, as supported electrocatalysts for PEMFCs and DMFCs.

#### ACKNOWLEDGEMENTS

The financial support of the Taiwan National Science Council is gratefully acknowledged.

#### References

1. S.H. Sun, G.X. Zhang, Y. Zhong, H. Liu, R.Y. Li, X.R. Zhou and X.L. Sun, *Chem. Commun.*, (2009) 7048.
2. F.J. Nores-Pondal, I.M.J. Vilella, H. Troiani, M. Granada, S.R. de Miguel, O.A. Scelza and H.R. Corti, *Int. J. Hydrogen Energy*, 34 (2009) 8193.
3. R.S. Amin, A.A. Elzatahry, K.M. El-Khatib and M.E. Youssef, *Int. J. Electrochem. Sci.*, 6 (2011) 4572.
4. F. Godínez-Salomón, E. Arce-Estrada and M. Hallen-López, *Int. J. Electrochem. Sci.*, 7 (2012) 2566.
5. H. Wang, S. Ji, W. Wang, V. Linkov, S. Pasupathi and R.F. Wang, *Int. J. Electrochem. Sci.*, 7 (2012) 3390.
6. J. Kim, S. Lim, S.K. Kim, D.H. Peck, B. Lee, S.H. Yoon and D. Jung, *J. Nanosci. Nanotechnol.*, 11 (2011) 6350.
7. S. Zhang, Y.Y. Shao, G.P. Yin and Y.H. Lin, *Appl. Catal. B: Environ.*, 102 (2011) 372.
8. R.I. Jafri, N. Sujatha, N. Rajalakshmi and S. Ramaprabhu, *Int. J. Hydrogen Energy*, 34 (2009) 6371.

9. R. Awasthi and R.N. Singh, *Int. J. Electrochem. Sci.*, 6 (2011) 4775.
10. A.Galal, N.F. Atta and H.K. Hassan, *Int. J. Electrochem. Sci.*, 7 (2012) 768.
11. F. Ye, X.R. Cao, L. Yu, S.Z. Chen and W.M. Lin, *Int. J. Electrochem. Sci.*, 7 (2012) 1251.
12. M.L. Lin, M.Y. Lo and C.Y. Mou, *J. Phys. Chem. C*, 113 (2009) 16158.
13. B. Ficicilar, A. Bayrakceken and I. Eroglu, *Int. J. Hydrogen Energy*, 35 (2010) 9924.
14. G. Gupta, D.A. Slanac, P. Kumar, J.D. Wiggins-Camacho, J. Kim, R. Ryoo, K.J. Stevenson and K.P. Johnston, *J. Phys. Chem. C*, 114 (2010) 10796.
15. S.H. Joo, K. Kwon, D.J. You, C. Pak, H. Chang and J.M. Kim, *Electrochim. Acta*, 54 (2009) 5746.
16. F. Hasche, T.P. Fellingner, M. Oezaslan, J.P. Paraknowitsch, M. Antonietti and P. Strasser, *ChemCatChem*, 4 (2012) 479.
17. S.H. Liu, R.F. Lu, S.J. Huang, A.Y. Lo, S.H. Chien and S.B. Liu, *Chem. Commun.*, (2006) 3435.
18. S.H. Liu, W.Y. Yu, C.H. Chen, A.Y. Lo, B.J. Hwang, S.H. Chien and S.B. Liu, *Chem. Mater.*, 20 (2008) 1622.
19. S.H. Liu, F.S. Zheng and J.R. Wu, *Appl. Catal. B: Environ.*, 108-109 (2011) 81.
20. S.H. Liu and J.R. Wu, *Int. J. Hydrogen Energy*, 36 (2011) 87.
21. S.H. Liu and S.C. Chen, *J. Solid State Chem.*, 184 (2011) 2420.
22. S.H. Liu, S.C. Chen and W.H. Sie, *Int. J. Hydrogen Energy*, 36 (2011) 15060.
23. Y. Wan, X. Qian, N. Jia, Z. Wang, H. Li and D. Zhao, *Chem. Mater.*, 20 (2008) 1012.
24. C. Liang and S. Dai, *J. Am. Chem. Soc.*, 128 (2006) 5316.
25. S.H. Liu, C.C. Chiang, M.T. Wu and S.B. Liu, *Int. J. Hydrogen Energy*, 35 (2010) 8149.
26. M.L. Lin, C.C. Huang, M.Y. Lo and C.Y. Mou, *J. Phys. Chem. C*, 112 (2008) 867.
27. Y.L. Hsin, K.C. Hwang and C.T. Yeh, *J. Am. Chem. Soc.*, 129 (2007) 9999.
28. T. Ramanathan, F.T. Fisher, R.S. Ruoff and L.C. Brinson, *Chem. Mater.*, 17 (2005) 1290.
29. A. Sarapuu, A. Kasikov, T. Laaksonen, K. Kontturi and K. Tammeveski, *Electrochim. Acta*, 53 (2008) 5873.
30. R.Z. Jiang, C. Rong and D. Chu, *Electrochim. Acta*, 56 (2011) 2532.
31. N.A. Anastasijevic, Z.M. Dimitrijevic and R.R. Adzic, *Electrochim. Acta*, 31 (1986) 1125.
32. N.M. Markovic, H.A. Gasteiger, B.N. Grgur and P.N. Ross, *J. Electroanal. Chem.*, 467 (1999) 157.
33. Z.X. Wu, Y.Y. Lv, Y.Y. Xia, P.A. Webley and D.Y. Zhao, *J. Am. Chem. Soc.*, 134 (2012) 2236.